ACS SyntheticBiology

pubs.acs.org/synthbio

Research Article

Orthogonal Blue and Red Light Controlled Cell−Cell Adhesions Enable Sorting-out in Multicellular Structures

Samaneh Rasoulinejad, Marc Mueller, Brice Nzigou Mombo, and Seraphine V. Wegner*

Cite This: *ACS Synth. Biol.* 2020, 9, 2076−2086

Read Online

ACCESS | Metrics & More | Article Recommendations | Supporting Information

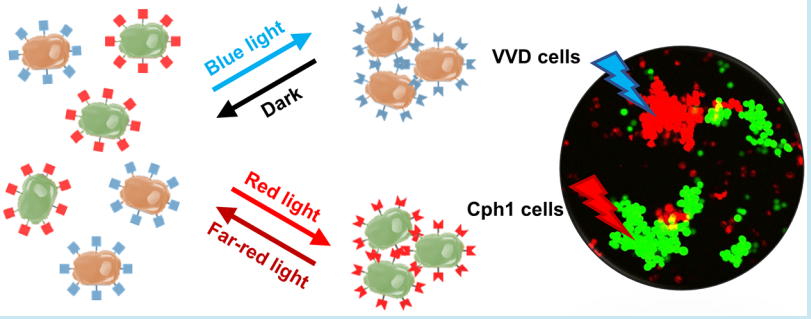

ABSTRACT: The self-assembly of different cell types into multicellular structures and their organization into spatiotemporally controlled patterns are both challenging and extremely powerful to understand how cells function within tissues and for bottom-up tissue engineering. Here, we not only independently control the self-assembly of two cell types into multicellular architectures with blue and red light, but also achieve their self-sorting into distinct assemblies. This required developing two cell types that form selective and homophilic cell−cell interactions either under blue or red light using photoswitchable proteins as artificial adhesion molecules. The interactions were individually triggerable with different colors of light, reversible in the dark, and provide noninvasive and temporal control over the cell−cell adhesions. In mixtures of the two cells, each cell type self-assembled independently upon orthogonal photoactivation, and cells sorted out into separate assemblies based on specific self-recognition. These self-sorted multicellular architectures provide us with a powerful tool for producing tissue-like structures from multiple cell types and investigate principles that govern them.

KEYWORDS: *self-sorting, multicellularity, cell−cell adhesions, photoswitchable, optogenetics*

During embryo development an initially symmetric multicellular structure undergoes spatiotemporally controlled morphogenic changes to self-organize into complex tissue architectures. At early stages, cells not only have the intrinsic capacity to self-assemble into multicellular structures, but different types of cells also self-sort into distinct patterns, which is the prerequisite for the proper formation of subsequent embryo architectures.[1,2] Even *in vitro* dissociated cells self-assemble into multicellular structures due to cell−cell adhesion and mixtures of cells derived from different tissues possess the remarkable ability to self-sort themselves into precise structures that resemble the tissues of origin.[3] In these multicellular structures cells are able to organize by distinguishing "self" from "non-self" based on differences in homophilic and heterophilic cell−cell adhesions.[4,5] In addition to the cellular arrangement, interactions between cells also fundamentally govern cell biology by communicating both biochemical and biophysical signals.[6,7] This is the reason why the misregulation of cell−cell adhesions is associated with diseases such as cancer, inflammation, and autoimmune diseases.[8,9] Furthermore, recent advances in organoid formation from different progenitor cell types[10] and the self-assembly of embryo mimetic structures from embryonic and extraembryonic stem cells[11,12] all demonstrate the enormous potential of multicellular architectures in regenerative medicine and synthetic biology.[13,14] Fundamentally, controlling when and where cell−cell adhesions of different types form is a major driving force in controlling the organization in multicellular structures and consequently their function.[15] Therefore, the approaches to control different types of cell−cell interactions independently with high spatiotemporal control are powerful becaue they comprise the assembly and self-sorting of cells into desired multicellular architectures from the bottom-up and understanding principles that govern multicellular architectures.[16]

Received: March 17, 2020
Published: July 1, 2020

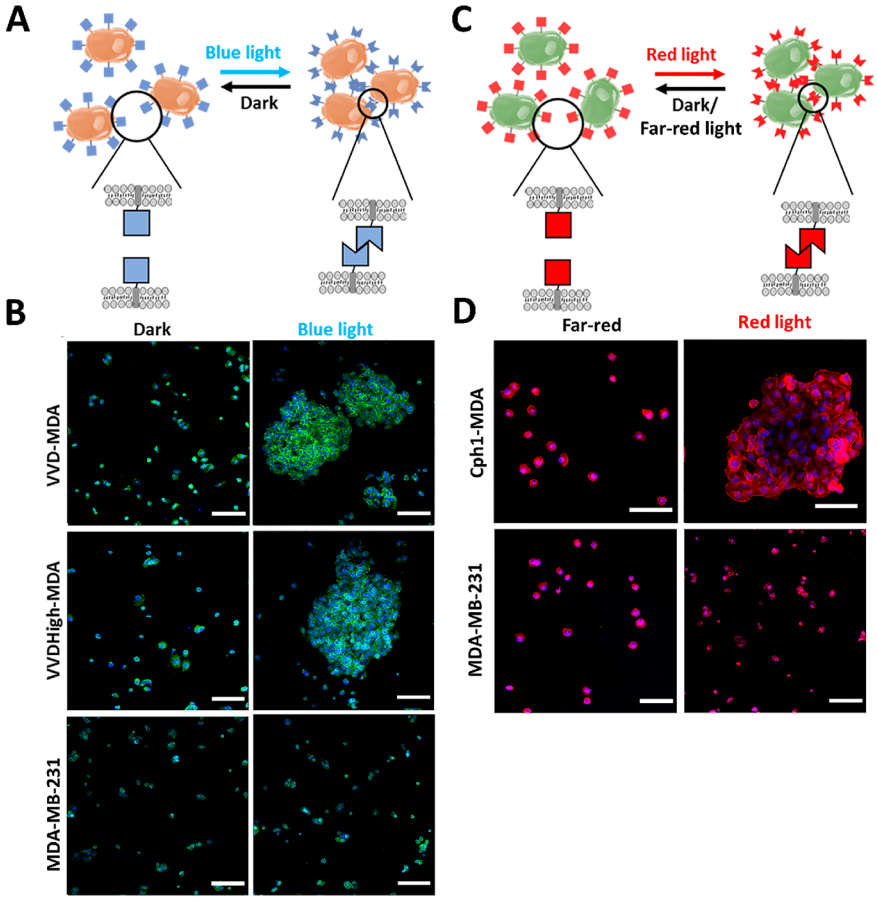

Figure 1. Blue and red light controlled cell−cell adhesions. (A) Cells expressing VVD or VVDHigh on their surfaces do not interact in the dark. Upon blue light illumination, the photoswitchable proteins on neighboring cells homodimerize and result in cell−cell adhesions. (B) VVD-MDA and VVDHigh-MDA cells grew as single cells in the dark and in large clusters under blue light 4 h after seeding in 2D culture at 8600 cells/cm^2. Green: actin phalloidin stain, blue: nuclear DAPI stain. (C) Cells expressing Cph1 on their surface do not interact with each other in the dark. Under red light, Cph1 proteins on neighboring cells homodimerize and lead to cell−cell adhesions. (D) Cph1-MDA cells grew as single cells under far-red and in large clusters under red light 4 h after seeding in 2D culture at 8600 cells/cm^2. Red, actin phalloidin stain; blue, nuclear DAPI stain. All scale bars are 200 μm. The nonmodified MDA-MB-231 cells used as negative control do not cluster independent of illumination.

Key prerequisites to achieve the desired self-assembly and self-sorting in multicellular structures include the independent control over different cell−cell adhesions within a mixture of different cell types. Up to now, both genetic[15,17] and chemical[18,19] approaches that alter the cell surface have been developed to regulate cell−cell adhesions for bottom-up tissue engineering and to further understand of the role of cell−cell adhesions in cell biology. It is possible to regulate the adhesiveness between different cell types by adjusting the expression of different native cell−cell adhesion receptors, such as cadherins,[4,5,15,20,21] and cells expressing different types of cadherins, aggregate separately when shaken in suspension, that is, sort out/self-sort.[4,22] However, it is not possible to locally alter cell interactions or reverse them at a desired point in time using this approach and even less so for multiple cell types. On the other hand, chemical reactive groups, formerly also used for self-assembly and self-sorting in colloidal systems, have been introduced onto the cell surfaces such as clickable groups,[18,19,23−25] single stranded DNA,[17,26−28] and supramolecular interaction partners.[9] All these synthetic cell−cell interactions provide some spatiotemporal regulation,[10] but suffer from dilution in the long term as the cells divide and poor reversibility and do not allow us to control multiple cell types in the same mixture. Consequently, these limitations neither enable self-sorting in multicellular mixtures, nor specifically manipulate different cell types in multicellular mixtures.

This study shows how we can regulate the adhesion of two different types of cells independently using blue or red light. For this purpose, we developed blue and red light switchable cell−cell interactions using photoswitchable proteins as artificial adhesion molecules enabling the assembly of desired multicellular structures by simply turning on the right color of light. We show how these cell−cell interactions can be used to independently and reversibly trigger both the self-assembly of each cell type and the self-sorting in a multicellular mixture. This study was inspired by a concept established with mixtures of two types of colloidal polystyrene particles, which could self-sort into distinct groups (also known as narcissistic or asocial self-sorting in the colloidal self-assembly community) using different colors of light.[29] In this study, we extend the concept of asocial self-sorting established for nonliving colloidal particles to cells for the assembly of multicellular tissue-like structures in the context of bottom-up tissue engineering. In this respect, this study is a demonstration of how well-established concepts of self-assembly and self-sorting for colloidal particles can be extended to multicellular systems

https://dx.doi.org/10.1021/acssynbio.0c00150
ACS Synth. Biol. 2020, 9, 2076−2086

and the parallels between self-sorting in colloidal mixtures and sorting-out in multicellular mixtures.

RESULT AND DISCUSSION

Design of Photoswitchable Homophilic Cell−Cell Adhesions. In the first step, we focused on engineering two different cell types that can be triggered with blue or red light independently to form homophilic cell−cell interactions. Our aim was to control each cell type using different colors of light as an external trigger to later address them separately in multicellular mixtures that self-sort. For this purpose, we expressed different photoswitchable proteins that homodimerize after exposure to light illumination as new adhesion receptors on the surfaces of cells. As photoswitchable cell adhesion receptors, we chose two different proteins that respond to different wavelengths: the blue light (450 nm) responsive protein LOV domain VVD from *Neurospora crassa*[30] and the red light (660 nm) responsive protein Cph1 phytochrome-like protein from *Cyanobactrium Synechocystis*.[31] Both of these proteins homodimerize upon light illumination and reversibly dissociate from each other in the dark as well as under far-red light (720 nm) for Cph1. Using these two molecularly orthogonal and independently addressable homophilic cell−cell interactions, we aimed to control the self-assembly and the self-sorting of each cell type individually (Figure 1A,C, Supporting Information, Figure S1). We assumed that cells expressing VVD on their surfaces would only interact with each other under blue light, but not under red light, and cells expressing Cph1 on their surfaces would only interact under red light, but not under blue light. Furthermore, we expected that under coillumination with blue and red light each cell type would sort itself out to form distinct clusters, analogous to the self-sorting behavior observed when two cell types expressing two different types of cadherins are mixed. The photoswitchable proteins used in this study form head-to-tail homodimers (i.e., the N-terminal of one protein binds to the C-terminal of the other protein) as shown by crystalography[23,32] and can mediate homophilic cell−cell interactions between neighboring cells that express the protein. Unlike other examples of artificial cell−cell adhesions, which form heterophilic cell−cell adhesion (interaction between cells of different types),[9,28,33,34] here presented cell−cell adhesions are homophilic. In this respect, the photoswitchable cell−cell interactions mirror the homophilic interaction mode of cadherin mediated cell−cell adhesions, but are different in terms of cell signaling as they do not have an intracellular tail to link to the cell cytoskeleton like cadherins. In addition, general advantages of photoregulation are the high spatiotemporal control, tunable dynamics, and high orthogonality without interference from other cellular processes, as previously demonstrated in numerous optogenetic studies.[33−39]

To generate photoswitchable cell−cell interactions, we first expressed the proteins VVD or Cph1 on the surfaces of cells. In our strategy, the photoswitchable proteins were cloned into the pDisplay plasmid with an N-terminal murine Ig κ-chain leader sequence, which directs the protein to the secretory pathway, and a C-terminal platelet derived growth factor receptor (PDGFR) transmembrane domain, which anchors the protein to the plasma membrane, displaying it on the extracellular side. Additionally, VVD variants and Cph1 were fused at their C-termini to the fluorescent tags mCherry and GFP (green fluorescent protein), respectively (Figure S2). Two variants of the VVD protein were used, VVD and VVD High, a mutant of VVD, which is a stronger homodimerizer and reverses slower in the dark.[30] These constructs were transfected into the breast cancer cell line MDA-MB-231, which was chosen because it does not express Type I cadherins and therefore does not form strong native cell−cell adhesions.[40] Stable monoclonal cell lines, expressing the photoswitchable proteins on their surfaces (VVD-MDA, VVDHigh-MDA, and Cph1-MDA) were isolated by fluorescence-activated cell sorting (FACS), and single clones with a high fluorescent signal were selected for future experiments (Figure S3A,C,E). The expression of the photoswitchable protein on the cell surface was confirmed by antibody staining of live cells without permeablization using flow cytometry and fluorescent microscopy (Figure S3B,D,F,G). Moreover, quantitative flow cytometry showed that 1×10^4 photoswitchable proteins per cell were expressed on the cell surface and the different photoswitchable proteins were expressed at similar levels (Figure S3H).

Blue and Red Light-Responsive Cell−Cell Interactions. In a first step, we investigated whether cells expressing the photoswitchable proteins VVD, VVDHigh, and Cph1 were able to form cell−cell interactions upon photoactivation under blue and red light, respectively. For this purpose, the cells were seeded in 2D culture on glass substrates at subconfluent densities (8600 cells/cm^2) and were incubated for 4 h in the dark (or far-red for Cph1-MDA) or under activating illumination (blue light for VVD- and VVDHigh-MDA, red light for Cph1-MDA). During this time, cell−cell interactions could form as the cells settled down and adhered to the glass surface. Subsequently, the cell nuclei and the actin cytoskeleton were stained to visualize the cell−cell interactions using the fluorescence microscopy. In the dark, VVD- and VVDHigh-MDA cells were evenly distributed over the substrate with few contacts between cells, and their morphology resembled the nontransfected MDA-MB-231 cells. In contrast, under blue light these cells grew in clusters and resembled cells, which form strong cell−cell adhesions (Figure 1B, Figure S4D,F). Similarly, Cph1-MDA distributed as single cells under far-red light, but formed large groups under red light illumination (Figure 1D, Figure S4E,G). Quantification of the light triggered clustering of VVD and Cph1 expressing cell lines in 2D further supported these observations (Figure S4A−C). In a control experiment with the parent MDA-MB-231 cell line, no light-dependent cell clustering was observed (Figure 1B,D). The results showed that VVD and Cph1 are suitable as adhesion receptors to form homophilic cell−cell interactions. Unlike approaches that rely on the chemical modification of cell surfaces to control cell−cell interactions, the genetically encoded optogenetic adhesion molecules guarantee stable expression on the cell surface as the cells were expanded and did not require constant cell surface modification.

Independent Photoactivation of VVD and Cph1 Mediated Cell−Cell Adhesions. In multicellular architectures, it is highly desirable to control different cell types independently. To demonstrate that the two different cell types that respond to blue and red light can be triggered without interference, we quantified the aggregation of cells expressing different photoswitchable proteins under different illumination conditions in suspension cultures. In suspension, cells expressing different photoswitchable proteins on their surfaces (5×10^4 cells/mL) were incubated on a 3D orbital shaker at

https://dx.doi.org/10.1021/acssynbio.0c00150
ACS Synth. Biol. 2020, 9, 2076−2086

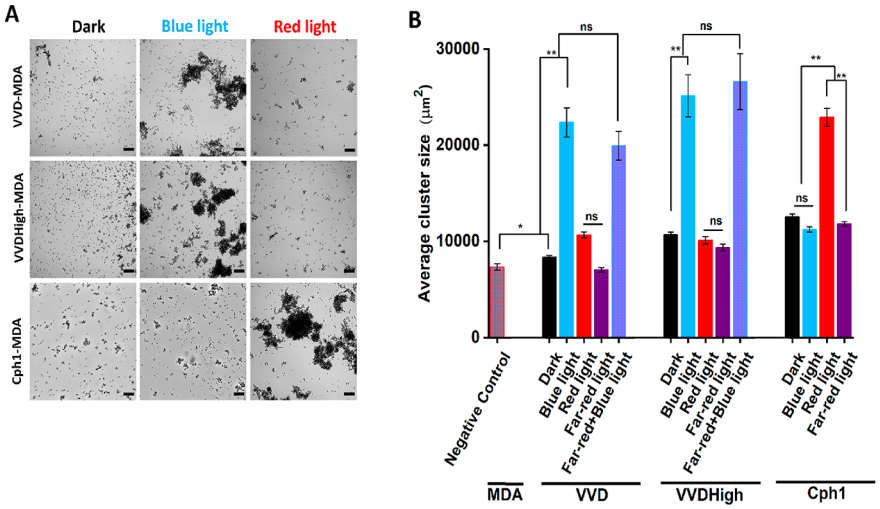

Figure 2. Independent control over cell−cell interactions with blue and red light. (A) Bright field images of cells expressing different photoswitchable proteins at their surface (5×10^4 cells/mL) incubated for 30 min on a 3D orbital shaker at 30 rpm in suspension under different illumination conditions. VVD-MDA and VVDHigh-MDA cells aggregated only under blue light and Cph1-MDA cells only under red light but not in the dark or illumination with the other color of light. Scale bars are 200 μm. (B) Quantification of the cell aggregation in suspension cultures. For each sample an area of 2.5 cm^2 (64 fields of view) was imaged using a tile scan and stitched together. All objects >5000 μm^2 (containing at least 20 cells) were identified as clusters. The quantification showed that cells aggregation was light specific and illumination with other wavelengths of light did not lead to significant clustering beyond the dark control. The background clustering of MDA-MB-231 cells (negative control) was lower than for the transfected cell types. Each experiment was performed in biological triplicate with two technical replicates each. Error bars are the standard error of the mean cluster area, $p \leq 0.05$ presented as an asterisk (*) and $p < 0.01$ presented as a double asterisk (**).

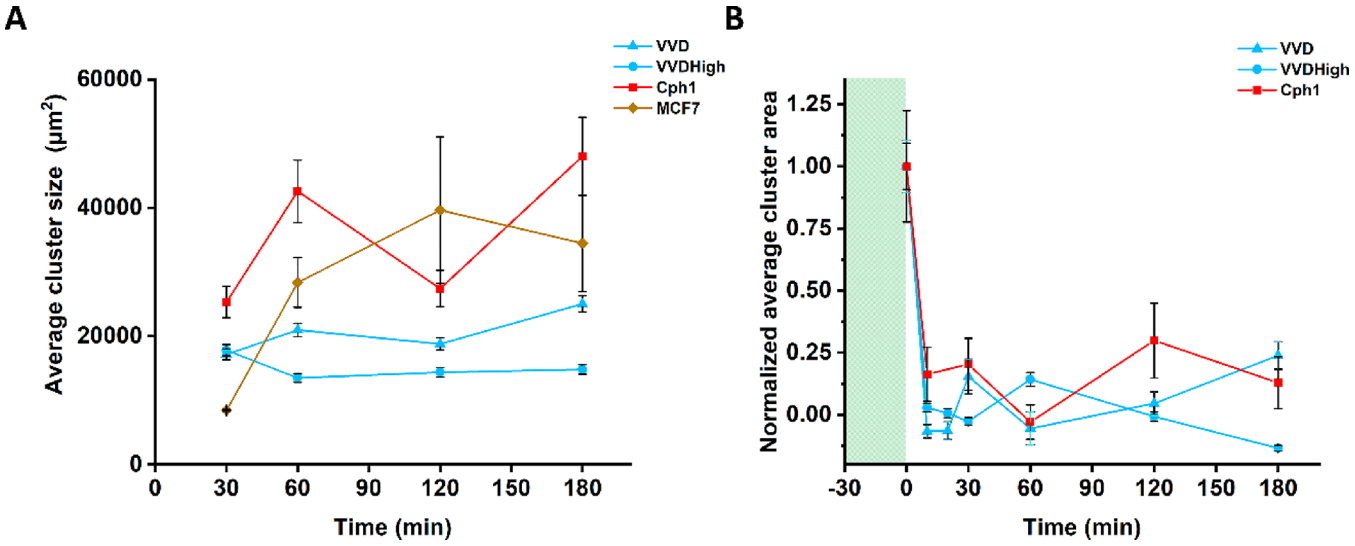

Figure 3. Light induced cell clustering and reversion kinetics. (A) Clustering of VVD-, VVDHigh-, and Cph1-MDA cells (5×10^4 cells/mL in suspension, 3D orbital shaker at 30 rpm) under photoactivation over time. MCF7 cells, which have high E-cadherin expression, were used as a positive control for cell clustering. (B) Reversibility of the light mediated cell−cell interactions in the dark for VVD- and VVDHigh-MDA cells, and far-red light for Cph1-MDA cells after 30 min prephotoactivation with appropriate light. The cluster area at each time point was normalized to the cluster area after 30 min photoactivation and 30 min in the dark. Error bars are the standard error of the mean. Each experiment was performed in biological duplicate with two technical replicates each.

30 rpm for 30 min in the dark, or either under far-red, blue, or red light illumination (Figure S5). Appropriate shaking was important to increase the likelihood of cells coming into proximity, allowing the formation of cell−cell interactions and preventing sedimentation; however, too high shear forces can also disrupt the clusters.[4] Microscopy images of the suspension cultures showed that the blue light responsive VVD- and VVDHigh-MDA cells remained mostly as single cells in the dark as well as under red and far-red light illumination, but formed large aggregates under blue light (Figure 2A and Figure S6A, tile scan image of the entire sample over 2.5 cm^2). On the other hand, red light responsive Cph1-MDA cells remained scattered in the dark as well as under far-red and blue light illumination, but assembled into aggregates under red light (Figure 2A). To support this qualitative observation of orthogonal response to blue and red light for VVD and Cph1 expressing cells, the aggregation was quantified by identifying clusters of cells (objects with an area >5000 μm^2, i.e., containing at least 20 cells) in the sample. This analysis showed that VVD- and VVDHigh-MDA as well as Cph1-MDA

https://dx.doi.org/10.1021/acssynbio.0c00150
ACS Synth. Biol. 2020, 9, 2076−2086

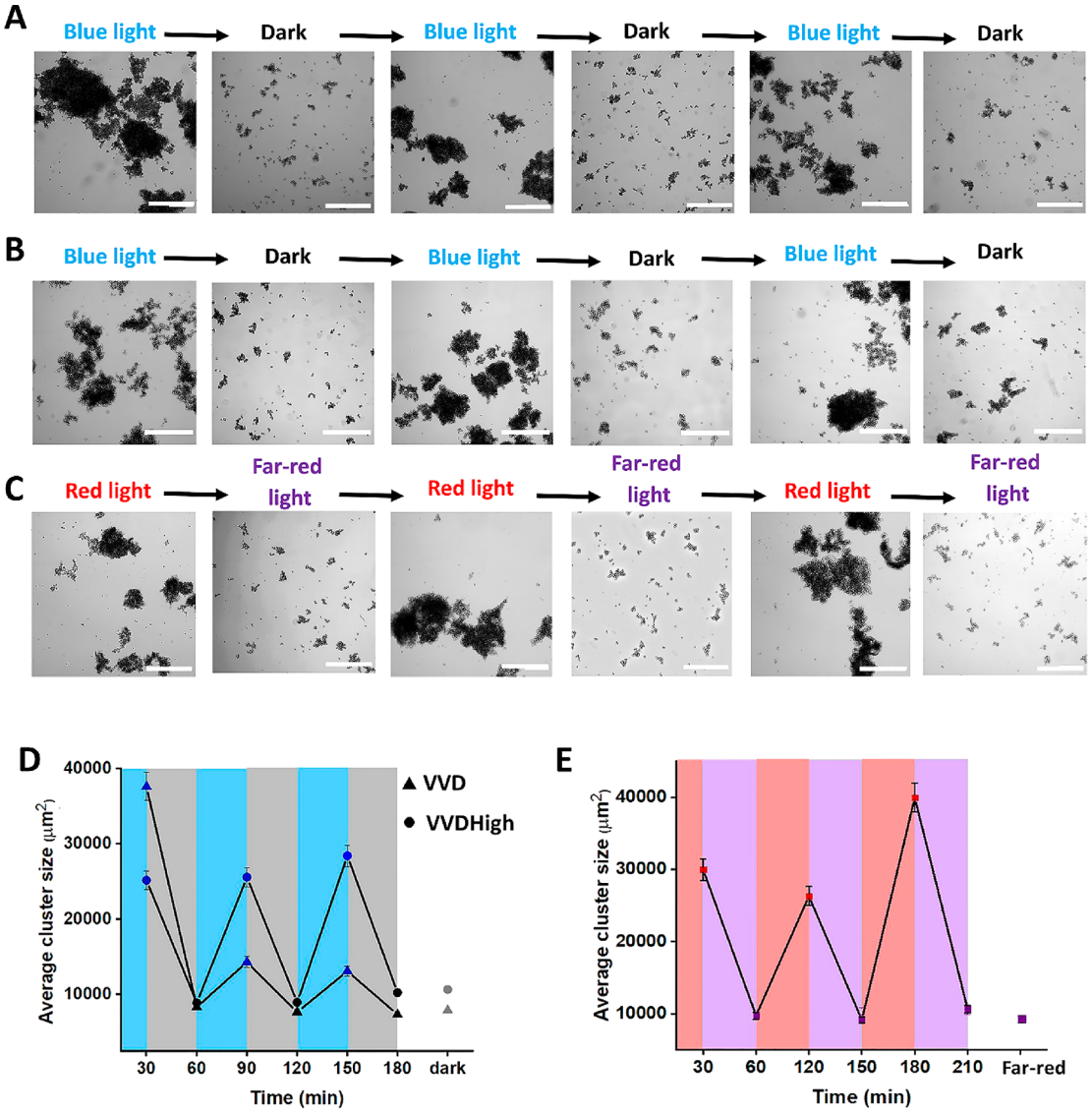

Figure 4. Reversibility of the photoswitchable cell−cell interactions. Bright field images of (A) VVD-MDA, (B) VVDHigh-MDA, and (C) Cph1-MDA cells in a suspension (5×10^4 cells/mL) altered between activating (30 min) and deactivating (30 min) conditions over multiple cycles. Scale bars are 300 μm. (D) Average cluster size for VVD-MDA (triangles) and VVDHigh-MDA (circles) over multiple blue light (blue points) /dark (black points) cycles. Blue and gray shaded backgrounds indicate 30 min periods where the blue light illumination was turned on and off, respectively. (E) Average cluster size for Cph1-MDA cells under altered illumination. Red and violet shaded backgrounds indicate 30 min periods under red (red square) and far-red (violet square) light, respectively. Cells were kept in the dark (VVD- and VVDHigh-MDA) or under far-red light (Cph1-MDA) as negative controls for the entire experiment. Both blue and red light dependent cell−cell interactions switched on and off over multiple cycles. For each sample an area of 2.5 cm^2 (64 fields of view) was imaged using a tile scan and stitched together. Each experiment was performed in biological triplicates with two technical replicates each. Error bars are the standard error of the mean.

cells formed similarly large clusters with an average projected area of ca. 23000 μm^2 upon photoactivation (Figure 2B, Figure S6B, cluster size distribution). Yet, for all three cell lines the aggregation in the dark or under illumination that does not activate the photoswitchable proteins was comparable to the background levels observed for the parent MDA-MB-231 cell (Figure 2B, S6A,B). Moreover, we also demonstrated that for VVD- and VVDHigh-MDA cells coillumination with far-red light, which deactivates Cph1-MDA cells, does not interfere with the blue light triggered clustering. It should also be noted that the blue and red light used had no toxic effect on the cells as confirmed by a cell viability assay (Figure S6C). Overall, this analysis showed that VVD/VVDHigh-MDA and Cph1-MDA cells formed cell−cell interactions only upon blue and red light illumination, respectively, and therefore can be triggered independently from each other without interference.

Dynamics and Reversibility of Light Responsive Cell−Cell Interactions. The reversibility and dynamics of cell−cell adhesions are important characteristics for their biological function, allowing cells to reorganize during morphogenesis and even allowing cells to break free of multicellular structures.[41,42] Tools that allow for such dynamic and reversible regulation of cell−cell interactions are therefore extremely valuable when it comes to investigating the importance of spatiotemporal regulation of cell−cell interactions.[9,33,34] For the here presented cell−cell interactions, we investigated the assembly and disassembly kinetics as well as

https://dx.doi.org/10.1021/acssynbio.0c00150
ACS Synth. Biol. 2020, 9, 2076−2086

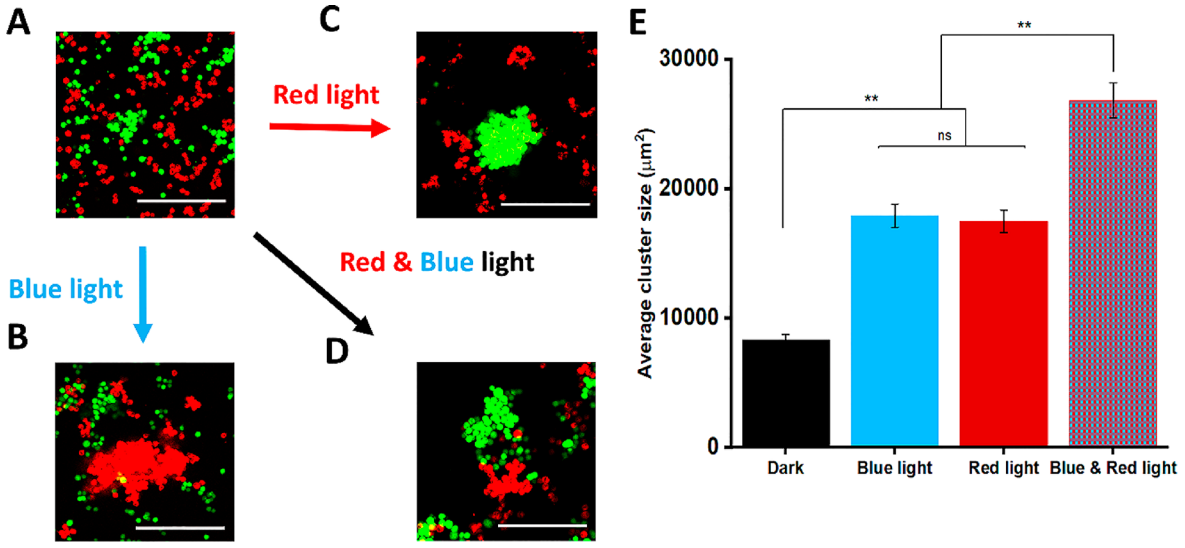

Figure 5. Blue and red light controlled self-assembly and self-sorting. Confocal images of VVD-MDA (red fluorescence channel) and Cph1-MDA (green fluorescence channel) mixed in a 1:1 ratio (A) in the dark, (B) under blue light, (C) under red light, and (D) under coillumination with blue and red light. Scale bars are 200 μm. (E) Average cluster size analysis of VVD-MDA and Cph1-MDA cells mixed in a 1:1 ratio under different illumination. For each sample an area of 2.5 cm^2 (64 fields of view) was imaged using a tile scan and stitched together. Each experiment was performed in biological triplicate with two technical replicates each. Error bars are the standard error of the mean, $p < 0.01$ presented as a double asterisk (**).

the repeated switchability of multicellular structures formed from blue and red light responsive cells.

When cell−cell interactions were photoactivated VVD-MDA, VVDHigh-MDA, and Cph1-MDA cells required different lengths of time to form aggregates in suspension cultures (Figure 3A). Under blue light, VVDHigh-MDA cells formed aggregates of maximal size within the first 30 min. The size of these aggregates then decreased to a certain extent over the next few hours, presumably due to compacting of the clusters. In contrast, VVD-MDA cells required 2.5 h under blue light to assemble into aggregates of a maximum size. Interestingly, while VVDHigh-MDA cells assembled faster than VVD-MDA cells, the VVD-MDA cells assembled into larger aggregates than VVDHigh-MDA cells. Cph1-MDA cells formed much larger multicellular assemblies under red light over the course of 3 h compared with cells expressing VVD proteins under blue light (ca. 2.5 fold). In fact, Cph1-MDA cells formed even larger clusters than MCF7 cells, which like MDA-MB-231 are a breast cancer cell line but with high E-cadherin expression. On the other side, cells expressing VVD proteins clustered less than MCF7 cells. Moreover, the cell clustering under light was faster for all photoswitchable proteins and already significant after 30 min, while the E-cadherin based clustering of MCF7 cells was slower and took over 1 h. These differences in assembly dynamics and final aggregate size could be explained by factors including the differences in intrinsic properties of the photoswitchable proteins, such as the thermodynamic and mechanical stability of the dimerization and the protein−protein interaction dynamics.[33]

An important feature of native cell−cell adhesions is their reversibility. Likewise, the cell−cell interactions mediated by the photoswitchable proteins were expected to be reversible due to the reversibility of the homodimerization of VVD in the dark and Cph1 under far-red light (Figure 3B). To confirm this, the different cell types (VVD-MDA, VVDHigh-MDA, and Cph1-MDA) were first aggregated under illumination that activated cell−cell adhesions for 30 min and subsequently placed in the dark for VVD- and VVDHigh-MDA, or under far-red light for Cph1-MDA cells. The aggregation analysis for all cell types showed that within 10 min of stopping the photoactivation most of the aggregates significantly disassembled and within 30 min the aggregation was comparable to cells that were not photoactivated (kept in the dark for VVD- and VVDHigh-MDA and under far-red light for Cph1-MDA for the entire duration of the experiment). Interestingly, the reversion kinetics for the different cell types were similar despite the different reversion kinetics of the photoswitchable proteins at the molecular level (VVD in dark $t_{1/2}$ = 2 h, VVD-High in dark $t_{1/2}$ = 4.7 h, Chp1 under far-red light $t_{1/2}$ = ca. milliseconds). The differences in reversion time at the molecular level and the cell−cell interactions show that it is not the reversion at the molecular level but other steps such as the separation of two cells from each other, the number of multivalent interactions, and the disassembly of the multicellular clusters that are the rate-determining steps. It should be noted that we have observed similar differences in the reversion kinetics at the molecular and the cell−cell adhesion level using other heterophilic light responsive protein−protein interactions.[33,34]

The reversibility of the blue and red light-triggered cell−cell adhesions allowed us to switch them on and off repeatedly. To check repeated switchability, suspensions of different cell types were alternated over three cycles between 30 min light activation and 30 min reversion. Bright field images acquired after each step showed that VVD- and VVDHigh-MDA cells associated into multicellular clusters every time they were incubated under blue light and dissociated from each other every time they were placed in the dark (Figure 4A,B). Similarly, Cph1-MDA cells associated and dissociated over multiple cycles when they were alternated between red and far-red light (Figure 4C). The quantitative analysis of the aggregation showed that for all three cell types reversion was complete each time the interactions were turned off following

https://dx.doi.org/10.1021/acssynbio.0c00150
ACS Synth. Biol. 2020, 9, 2076−2086

photoactivation. Further, in VVD-MDA cells the amount of aggregation decreased in the second and third blue light activation cycle compared to the first light activation, which indicates partial fatigue (Figure 4D). In contrast, VVDHigh-MDA and Cph1-MDA cells aggregated equally well after each illumination cycle and showed no fatigue, that is, no change in aggregation over multiple cycles (Figure 4D,E). Overall, both the blue and red light switchable cell−cell interactions were reversible and could be switched on and off repeatedly, which captures important properties of cell−cell interactions.

Light Specific Self-Sorting in Multicellular Mixtures. Finally, we explored whether we could control self-sorting in multicellular mixtures and address different cell types within the mixture independently after exposure to blue and red light. For this purpose, we mixed equal numbers of VVD-MDA (labeled with a red fluorescent dye) and Cph1-MDA (labeled with a green fluorescent dye) cells and observed their assembly either under blue or red light or coillumination with both colors of light after 30 min incubation. In the dark, the two cell types were well dispersed (Figure 5A) and their self-assembly was inducible for one cell type at a time using two different wavelengths of light. Under blue light, VVD-MDA cells assembled into clusters, which were observable as large red fluorescent aggregates, and Cph1-MDA cells labeled in green remained dispersed (Figure 5B). Conversely, under red light, only Cph1-MDA cells self-assembled into large aggregates, observed as large green fluorescent objects, whereas VVD-MDA cells remained more scattered (Figure 5C). Most remarkably, the simultaneous illumination with blue and red light, resulted in the self-sorting of VVD-MDA and Cph1-MDA cells into distinct green and red fluorescent cell clusters with almost no intermixing of the two cell types within the same cluster (Figure 5D, Figure S7). The sorting out of the two cell types was also confirmed by 3D confocal microscopy cross sections of the clusters (Figure S7A−C). Further, colocalization analysis of green and red labeled cells showed that the two cell types separated into individual clusters (Figure S9). The qualitative observations of light specific cell-sorting were further supported by quantitative aggregation analysis in mixed VVD-MDA and Cph1-MDA cultures based on bright field microscopy images as described above (Figure 5E). In the 1:1 mixed VVD-MDA and Cph1-MDA cultures, the aggregation increased both upon blue or red light illumination when compared to experiments in the dark. Moreover, the amount of aggregation doubled under coillumination with blue and red light compared to illumination with just one color of light, as both cell types were photoactivated. It should be noted that the labeling with the fluorescent dyes had no effect on the cell aggregation under light activation (Figure S9).

CONCLUSION

Overall, these findings show that within a mixture of two different cell types, the assembly of multicellular structures can be triggered independently using blue and red light for VVD-MDA and Cph1-MDA cells, respectively. Further, the high specificity of the homodimerizations of VVD and Cph1 provide molecularly orthogonal cell−cell interactions and make it possible to achieve self-sorting within a multicellular mixture. Previously, DNA and supramolecular interactions first used in colloidal assembly[43,44] were implemented onto cells to assemble multicellular structures. The parallels between colloidal and cellular self-assembly are also witnessed by *in vitro* bead aggregation assays with cadherin coated beads.[45] Transferring the recently reported sorting out behavior (known as narcissistic or asocial self-sorting in the colloidal self-assembly community) achieved with mixtures of VVDHigh and Cph1 coated polystyrene beads[29] to cells shows that not just concepts in colloidal self-assembly but self-sorting also apply to multicellular structures. The comparable self-assembly and self-sorting observed in synthetic colloidal systems and in multicellular mixtures shows that these photoswitchable proteins provide a transferable framework to produce higher order architectures and achieve self-sorting of micrometer sized objects.

The possibility of triggering different cell−cell interactions within a multicellular assembly using different colors of light offers many opportunities in the bottom-up assembly of diverse cell types into tissue-like structures and understanding the principles behind self-organization during development. The remarkable and innate ability of cells to self-assemble and sort themselves out into tissue-like architectures reveal the high potential of bottom-up tissue engineering and make controlling cell−cell adhesions a very powerful tool to program synthetic tissues.[11,12,15] In this study, we have demonstrated how we can control the assembly and self-sorting of one cell type independently in the presence of another cell type relying on orthogonal triggers (i.e., blue and red light) and orthogonal molecular interactions (VVD and Cph1). These photoswitchable proteins can be integrated into different types of cells with diverse genetic backgrounds as they are genetically encodable. The reversibility of the photoswitchable cell−cell adhesions makes it possible to bring certain cells in contact for a desired time and later remove the interactions. On the other hand, depending on the cell type secondary interactions between cells, endogenous cell adhesion molecules and extracellular matrix molecules could lead to the further stabilization of multicellular structures even if illumination is stopped. In this study, we have only temporally controlled cell−cell adhesions using different illumination but photoregulation in general also allows for spatial control through local illumination and tuning of interactions by altering illumination intensity and frequency. These features of the photoswitchable cell−cell adhesion open the door for building more complex and programmable tissues from cellular building blocks.

The photoswitchable cell−cell interactions further provide a unique chance of investigating the cell biology related to cell−cell interactions. Just like the native cadherin of cell−cell adhesions, the VVD and Cph1 mediated cell−cell adhesions also generate artificial adhesions between the same types of cells. Initial cell clustering analysis showed that especially Cph1-MDA cells could form equally large multicellular aggregates as MCF7 cells, which express high levels of E-cadherin. This finding suggests that the opto-adhesion molecules are comparable to native adhesion molecules but an exact comparison in terms of adhesion strength and dynamics as well as their compatibility requires further investigation. Moreover, the photoswitchable cell−cell adhesions like native cell−cell adhesions are switchable and dynamic, and can potentially be tuned and spatiotemporally controlled as it is often the case during many biological processes. Differently from the cadherin-based cell−cell interaction these photoswitchable cell−cell interactions do not link to the actin cytoskeleton and the associated signaling pathways. This fact provides a unique tool to dissect

https://dx.doi.org/10.1021/acssynbio.0c00150
ACS Synth. Biol. 2020, 9, 2076−2086

biochemical from biophysical signals transduced by cell−cell adhesions. More generally, these findings suggest that it is possible to assemble multicellular structures from cells and control parts of them with blue and red light switchable cell−cell interaction pairs. Analogous to the sorting out of cells that express different cadherins types, cells expressing blue and red light-switchable surface proteins were able to replicate the same self-sorting behavior. Future studies that take advantage of the spatiotemporal control that photoregulation provides will allow the assembly of new multicellular structures and the study of related questions in cell biology.

MATERIALS AND METHODS

Constructs and Sequences. The VVD and the Cph1 gene were synthesized in the pET-21b(+) plasmid between the NdeI-XhoI and NdeI-*Sal*I cutting sites, respectively, by Genscript. The VVDHigh was derived from VVD by point mutations using Agilent kit (Site-Directed Mutagenesis kit, Catalog #200523). In a first step, mCherry and GFP were cloned into the pDisplay mammalian expression vector (Invitrogen V66020) between the Ig κ-chain leader sequence and the platelet derived growth factor receptor (PDGFR) domain using Gibson cloning with the primers listed in Table S1 to yield mCherry-pDisplay and GFP-pDisplay, respectively. In a second step, the photoswitchable proteins VVD- and VVDHigh were cloned into mCherry-pDisplay and Cph1 into GFP-pDisplay between the Ig κ-chain leader sequence and the fluorescent proteins. The pDisplay plasmid (Invitrogen) fuses the photoswitchable protein and the fluorescent protein at the N-terminal to the murine Ig κ-chain leader sequence, which directs the protein to the secretory pathway and at the C-terminal to the platelet-derived growth factor receptor (PDGFR) transmembrane domain, which anchors the proteins on the extracellular part of the plasma membrane. Moreover, the pDisplay plasmid contains a myc-epitope on the extracellular part to detect the expression of surface proteins.

Cell Culture. All cells were cultured in DMEM (Dulbecco's Modified Eagle Medium)/F12 (1:1) (Gibco) supplemented with 10% FBS (fetal bovine serum, Gibco) and 1% penicillin/streptomycin at 37 °C and 5% CO_2. MDA-MB-231 cells were transfected using lipofectamin 3000 (ThermoFisher, L300001) following the manufacturer's protocol for a 6-well plate. After 24 h, the cell culture medium was supplemented with 1800 μg/mL G418 (Geneticin, Roche), and cells were maintained with G418 for all further experiments. After culturing the cells for 2 weeks with G418 selection, the transfected cells were sorted at the core facility of the Institute of Molecular Biology (IMB) in Mainz using BD FACS Aria III Cell sorter into a 96-well plate with one cell per well. After expanding monoclonal cultures, their fluorescence was measured again by flow cytometry (Attune NXT Acoustic Focusing Cytometer, Invitrogen). The clones with the highest fluorescent signal among all sorted cells were selected for future experiments.

Flow Cytometry Analysis for the Detection of Surface Protein Expression. Cells were washed with phosphate buffer saline (PBS). Afterward the cells were detached with accutase (Gibco, Catalog #A1110501) and subsequently washed twice with ice-cold PBS. Subsequently, 1×10^6 cells were resuspended in 100 μL of 10 μg/mL of the primary antibody rabbit anti-c-myc (Invitrogen, catalog #700648) in PBS and incubated at 4 °C while being gently mixed for 45 min. Then, the cells were washed three times by adding 900 μL of cold PBS to the cells and thereafter harvested by centrifugation (400*g*, 4 °C for 5 min). VVD-MDA and VVDHigh-MDA cells were resuspended in 100 μL of 10 μg/mL Alexa 488 goat antirabbit IgG (Invitrogen, catalog #A27034) and Cph1-MDA cells were resuspended in 100 μL of 10 μg/mL of Alexa 594 goat antirabbit IgG (Invitrogen, catalog #A-11037) and incubated at 4 °C while being gently mixed for 30 min. The cells were washed three times with 900 μL of cold PBS and finally resuspended in 500 μL of cold PBS. The cells were analyzed using flow cytometry (Invitrogen, Attune NxT Flow Cytometer) and each analysis contained at least 10 000 gated events. Rabbit-IgG (Invitrogen, catalog #11-4614-80) was used as a primary antibody isotype control to assess the background signal.

Quantification of Protein Expression on the Cell Surfaces. Cells were cultured overnight, 5×10^5 cells per t25-flask with 5 mL of medium. The next day, all cells (VVD-, VVDHigh-, Cph1- MDA, and MDA-MB-231) were washed with PBS, detached with accutase and then washed with ice-cold PBS twice. A million cells from each cell type were incubated with 10 μg/mL rabbit anti-c-myc (Invitrogen, catalog #700648) in 100 μL of PBS at 4 °C for 45 min while gently mixing. Then, the cells were washed three times with 900 μL of cold PBS and harvested after each step by centrifugation (400*g*, 4 °C for 5 min). The cells were resuspended in 100 μL of 10 μg/mL Alexa 488 goat antirabbit IgG (Invitrogen, catalog #A27034) and incubated at 4 °C for 45 min while being gently mixed. The cells were washed three times with 900 μL of cold PBS and finally resuspended in 200 μL of cold PBS. The cells were analyzed using flow cytometry (Invitrogen, Attune NxT Flow Cytometer). The Quantum Alexa Fluor 488 MESF kit (Bang Laboratories, Inc., 488A) was used for quantification following the manufacture's protocol. The median of fluorescence peak from each cell type was measured and converted into MESF (molecules of equivalent soluble fluorochrome) based on the calibration curve generated using the QuickCal v.2.4 software from Bang Laboratories. The MESF of same cell type (negative control) that was not incubated with antibodies and MESF for MDA-MB-231 cells incubated with antibodies was subtracted for final calculation of specific MESF of each cells type.

Immunostaining for the Detection of Surface Protein Expression. VVD-MDA, VVDHigh-MDA, and Cph1-MDA cells were seeded on μ-Slide 4 Well Glass Bottom (ibidi, catalog #80427) at 2×10^5 cell/well and cultured overnight. The cells were washed three times with PBS and blocked with 1% BSA (bovine serum albumin) in HBSS (Hank's Balanced Salt Solution, Gibco, Catalog #14025050) for 20 min. Afterward, the cells were stained with the primary antibody rabbit anti-c-myc (Invitrogen, catalog #700648) diluted in HBSS 1:500 and incubated for overnight at 4 °C. Cells were washed three times with cold HBSS, fixed with 2% PFA (paraformaldehyde) in HBSS at room temperature for 10 min and subsequently blocked with 1% BSA for 10 min. The cells were stained with a fluorescently labeled secondary goat antirabbit antibody (Alexa488 labeled for VVD-MDA and VVDHigh-MDA and Alexa594 labeled for Cph1-MDA cells), diluted 1:1000 in HBSS then incubated overnight at 4 °C. The cells were washed four times with HBSS and the nuclei were stained with Hoechst 33342 (Invitrogen, catalog #H3570), diluted to 1:1000, and incubated for 10 min at room temperature. Confocal images were acquired with a 153.6 μm pinhole in the Hoechst 33342, Alexa488, and Alexa594 channels on a laser scanning confocal microscope (Leica SP8)

https://dx.doi.org/10.1021/acssynbio.0c00150
ACS Synth. Biol. 2020, 9, 2076−2086

equipped with 405, 488, and 552 nm laser lines and a 20×/0.95 air objective to detect the nuclei, the transfected protein using the c-myc epitope, and the protein expression in the fluorescent protein channel (mCherry-tag for VVD and VVDHigh and GFP-tag for Cph1).

Light-Responsive Cell−Cell Interactions in 2D. All cells were washed with PBS and detached with accutase for 10 min at room temperature. Thereafter, for 2D culture experiments cells were seeded at a cell density of approximately 8600 cells/cm^2 on 24 mm × 24 mm cover glass slides. The LED light module V10 with TS-110 Controller (CLF Plant Climatics GmbH) was used in this experiment, and dark samples were wrapped in aluminum foil (Figure S11). VVD- and VVDHigh-MDA cells were cultured in the presence of 0.5 μM FAD (flavin adenine dinucleotide) and cultured either in the dark or under blue light (463 nm, 20.4 μW/cm^2) for 4 h at 37 °C and 5% CO_2. Cph1-MDA cells were cultured in the presence of 5 μM of PCB (phycocynobilin) and cultured either under far-red light (734 nm, 25.2 μW/cm^2) or under red light (620 nm, 23.2 μW/cm^2) for 4 h at 37 °C and 5% CO_2. Moreover, in clustering experiments MDA-MB-231 and MCF7 cells were used as a negative and positive controls, respectively, and were handled as the transfected cells.

All cells were fixed with 2% PFA in PBS for 15 min at room temperature, permeabilized with 0.1% Triton-X-100 in PBS for 5 min and the actin cytoskeleton was stained with Phalloidin-iFlour 488 reagent (Abcam, ab176753) for VVD- and VVDHigh-MDA cells, and Phalloidin-iFlour 594 reagent (Abcam, ab176757) for Cph1-MDA cells according to manufacture protocol. Subsequently, the cells were mounted with mowiol containing 1 μg/mL DAPI (4′,6-diamidine-2′-phenylindole dihydrochloride) for nuclear staining. Fluorescence images were acquired in the TRITC, FITC, and DAPI channels in a tile scan of an area of 1 cm^2 on an inverted fluorescence microscope (Leica DMi8) through a 5× air objective.

For the cell clustering analysis 2D cultures the number of cells was quantified based on the DAPI staining and the number of cells growing in clusters was quantified based on the actin staining using CellProfiler 2.2.0[46] and MATLAB. In the actin channel, objects with an area >300 μm^2 were classified as cells, objects with an area of 300−3000 μm^2 as single cells, and objects with an area >10000 μm^2 as clusters of cells, as described previously.[34]

Light-Dependent Aggregation in Suspension Cultures. All cell types were detached using accutase, resuspended at 5 × 10^4 cell/mL in DMEM/F-12 without phenol red + *L*-glutamine containing 25 mM of HEPES (4-(2-hydroxyethyl)-1-piperazineethanesulfonic acid), and 1 mL aliquots were added into 1.5 mL LoBind microfuge tubes (Eppendorf). In addition, the medium was supplemented with 0.5 μM FAD for VVD- and VVDHigh-MDA cells and 5 μM of PCB for Cph1-MDA cells. Afterward, cells were illuminated with red (620 nm, 1440 μW/cm^2), far-red light (734 nm, 1120 μW/cm^2), blue light (463 nm, 544 μW/cm^2) (Figure S4) and in the dark (wrapped in aluminum foil) for 30 min on the 3D orbital shaker at 30 rpm at room temperature. LED grow light panels (Albrillo) were used in this experiment, with one and two neutral-density filter for blue and red light, respectively. The neutral-density filter was used to minimize the scattered light of the light panel. Each neutral-density filter reduced 50% of the light intensity. The whole 1 mL suspension of cells was fixed with 500 μL of 4% PFA in PBS after incubation under light or in the dark and was transferred to a 12-well plate. Bright field images were acquired for a total area of 2.5 cm^2 (8 × 8 tile scan images; imaged area, 2.5 cm^2) using an inverted fluorescence microscope (Leica DMi8) with a 5× air objective. Images were analyzed with Fiji 1.52d. The bright field of 8 × 8 tile scan images were individually background corrected for uneven illumination and for dirt/dust on the lenses by using a pseudo flat field correction with a blurring stack of five and merged into a single image. The area of individual cell clusters was determined using a particle analysis tool and clusters were defined as objects >5000 μm^2, which corresponds to a projection area of at least 20 cells (the area for a single cell is equal to 200−250 μm^2). For automated image analysis a macro script was written, which can be found in the Supporting Information.

The area of individual cell clusters and the mean cluster area were calculated using OriginPro2019. Each experiment was performed in biological triplicate with two technical replicates ($n = 3 \times 2$). The data are presented as the mean cluster area ± SE for clusters detected in all experiments. The Mann−Whitney test was performed to analyze the statistical difference. $p > 0.1$ ns, $p \leq 0.05$ presented as an asterisk (*), $p < 0.01$ presented as a double asterisk (**) and $p < 0.001$ presented as a triple asterisk (***).

Dynamics and Reversibility of Blue and Red Light-Triggered Cell−Cell Interactions. The assembly and disassembly kinetics as well as the repeated on/off switching of cell−cell interactions were evaluated in suspension cultures as described above with variations in the illumination protocols. For the assembly kinetics, the cells were placed under illumination (blue light for VVD-MDA and VVDHigh-MDA, red light for Cph1-MDA) for up to 4 h before fixing the cells. To access the reversion kinetics, cells were first activated for 30 min under illumination and subsequently placed in the dark for VVD-MDA and VVDHigh-MDA, and far-red light for Cph1-MDA cells. For the repeated on/off switching VVD-MDA and VVDHigh-MDA cells were alternated between 30 min blue light and 30 min in the dark, and Cph1-MDA cells were alternated between 30 min red light and 30 min far-red light. After each point in time two samples were fixed with PFA and analyzed as described above.

Self-Sorting in Mixed Cell Populations. VVD-MDA and Cph1-MDA in suspension were stained with CellMask Deep Red Plasma Membrane (Invitrogen, C10046) and CellTracker Green CMFDA Dye (Invitrogen, C2925), respectively, using a 1:1000 dilution of each dye and incubating them at 37 °C for 30 min, while mixing the cells every 10 min. The cells were covered with aluminum foil to protect them from light. The cells were then centrifuged at 400*g* for 5 min, the medium was discarded, and cell pellets were resuspended in DMEM/F12 medium supplemented with 25 mM HEPES, 0.5 μM FAD, and 5 μM PCB. The stained VVD-MDA and Cph1-MDA were mixed in a 1:1 ratio in total 1 × 10^5 cell/mL density in a total volume of 1 mL in 1.5 mL Lobind tubes, and the cell mixtures were illuminated with blue light, red light, blue and red light, or kept in the dark for 30 min on the 3D orbital shaker at 15 rpm at room temperature. The cells were fixed with 500 μL of 4% PFA and fluorescent images were acquired on a confocal microscope. The same experiment was repeated with unstained cells, and after fixation bright field images were acquired for aggregation analysis. To exclude the effect of staining on the cell clustering, the cell clustering experiments were performed

https://dx.doi.org/10.1021/acssynbio.0c00150
ACS Synth. Biol. 2020, 9, 2076−2086

with stained and unstained VVD-MDA and Cph1-MDA cells under blue and red light, respectively.

Colocalization Analysis. The confocal images of the self-sorting were analyzed by using imagJ and the plugin EzColocalization.[47] The images in the red and green fluorescent channels were loaded into the EzClocalization and the colocalization of the two fluorescent signals was analyzed using the TOS (threshold overlap score, linearly rescaled) and PCC (Pearson's correlation coefficient) with 10% FT (top percentage of pixels threshold). Both for TOS and PCC, values of −1 represent complete anticolocalization, values of 0 represent no colocalization, and values of 1 represent complete colocalization.[47,48]

Light Toxicity. VVD-MDA and Cph1-MDA cells were prepared as for light-dependent aggregation studies at 5×10^4 cells in a total volume of 1 mL media in 1.5 mL Lobind tubes and incubated under illumination or in the dark for 30 min. Subsequently, 100 μL of medium containing cells was transferred to a 96-well plate. The viability of the cells was measured using the CellTiter-Glo2.0 Assay (Promega) according to manufacturer's instructions.

Statistical Analysis. All the experiments were performed with 2 techniques in 3 biological replications. The statistical analyses were determined using a nonparametric test by the two-independent samples Mann−Whitney test. All the data are shown as mean ± SE. In box plots each box is defined as the 25th and 75th percentile of the data, the line in the box represents the median, the dots the mean, and whiskers the 10th and 90th percentiles. The significant level was set at $P < 0.01$. The groups with "ns" have no significant differences. OriginPro software version 2019 (OriginLAb, Corporation, Northampton, MA, USA) was used for all analyses.

■ ASSOCIATED CONTENT

Supporting Information

The Supporting Information is available free of charge at https://pubs.acs.org/doi/10.1021/acssynbio.0c00150.

> Scheme of orthogonal blue and red light triggered self-sorting, details of the designed protein constructs, quantification of surface protein expression by flow cytometry and immunostaining, spectra of the used light sources, quantification of light triggered cell clustering in 2D cultures, evaluation of light toxicity, tile scan bright field images of suspension cultures and evaluation of cell cluster size under different illumination conditions, confocal z-stack images and colocalization analysis in self-sorting multicellular mixtures, effect of cell staining on light triggered cell clustering, and primer sequences (PDF)

■ AUTHOR INFORMATION

Corresponding Author

Seraphine V. Wegner − *Max Planck Institute for Polymer Research, Mainz 55128, Germany; Institute of Physiological Chemistry and Pathobiochemistry, University of Münster, Münster 48149, Germany;* orcid.org/0000-0002-9072-0858; Email: wegnerse@exchange.wwu.de

Authors

Samaneh Rasoulinejad − *Max Planck Institute for Polymer Research, Mainz 55128, Germany*

Marc Mueller − *Max Planck Institute for Polymer Research, Mainz 55128, Germany*

Brice Nzigou Mombo − *Institute of Physiological Chemistry and Pathobiochemistry, University of Münster, Münster 48149, Germany*

Complete contact information is available at: https://pubs.acs.org/10.1021/acssynbio.0c00150

Author Contributions

S.R. and S.W. designed the experiments, S.R. conducted the experiments and analyzed the data. M.M. supported S.R. during cell sorting and image analysis. S.R. and B.N. helped with the quantification of protein expression MCF7 cells clustering. S.R. and S.V.W. wrote the manuscript. All authors reviewed the results and approved the final version of the manuscript.

Funding

This work was funded by the European Research Council ERC Starting Grant ARTIST (#757593).

Notes

The authors declare no competing financial interest.

Data and materials availability. All data needed to evaluate the conclusions in the paper are present in the paper and/or the Supporting Information. Additional data related to this paper may be requested from the authors.

■ ACKNOWLEDGMENTS

We would like to thank Dr. Stefanie Möckel and Dr. Jesús Gil Pulido at IMB Flow Cytometry Core Facility (FCCF) for support with FACS measurements, Dr. Carole Champanhac and Andreas Best for their technical assistance, and Stefan Schuhmacher for graphical support.

■ REFERENCES

(1) Foty, R. A., and Steinberg, M. S. (2004) Cadherin-Mediated Cell-Cell Adhesion and Tissue Segregation in Relation to Malignancy. *Int. J. Dev. Biol. 48*, 397−409.

(2) Steinberg, M. S., and Poole, T. J. (1981) Strategies for Specifying Form and Pattern: Adhesion-Guided Multicellular Assembly. *Philos. Trans. R. Soc., B 295*, 451−460.

(3) Steinberg, M. S. (1963) Reconstruction of Tissues by Dissociated Cells. Some Morphogenetic Tissue Movements and the Sorting out of Embryonic Cells May Have a Common Explanation. *Science 141*, 401−408.

(4) Duguay, D., Foty, R. A., and Steinberg, M. S. (2003) Cadherin-Mediated Cell Adhesion and Tissue Segregation: Qualitative and Quantitative Determinants. *Dev. Biol. 253*, 309−323.

(5) Thu, C. A., Chen, W. V., Rubinstein, R., Chevee, M., Wolcott, H. N., Felsovalyi, K. O., Tapia, J. C., Shapiro, L., Honig, B., and Maniatis, T. (2014) Single-Cell Identity Generated by Combinatorial Homophilic Interactions between Alpha, Beta, and Gamma Protocadherins. *Cell 158*, 1045−1059.

(6) Hui, E. E., and Bhatia, S. N. (2007) Micromechanical Control of Cell−Cell Interactions. *Proc. Natl. Acad. Sci. U. S. A. 104*, 5722−5726.

(7) Wei, Q., and Huang, H. (2013) Insights into the Role of Cell−Cell Junctions in Physiology and Disease. *Int. Rev. Cell Mol. Biol. 306*, 187−221.

(8) Ryan, P. L., Foty, R. A., Kohn, J., and Steinberg, M. S. (2001) Tissue Spreading on Implantable Substrates Is a Competitive Outcome of Cell-Cell vs. Cell-Substratum Adhesivity. *Proc. Natl. Acad. Sci. U. S. A. 98*, 4323−4327.

(9) Shi, P., Ju, E., Yan, Z., Gao, N., Wang, J., Hou, J., Zhang, Y., Ren, J., and Qu, X. (2016) Spatiotemporal Control of Cell−Cell Reversible Interactions Using Molecular Engineering. *Nat. Commun. 7*, 13088.

(10) Stephan, M. T., and Irvine, D. J. (2011) Enhancing Cell Therapies from the Outside In: Cell Surface Engineering Using Synthetic Nanomaterials. *Nano Today 6*, 309−325.
(11) Harrison, S. E., Sozen, B., Christodoulou, N., Kyprianou, C., and Zernicka-Goetz, M. (2017) Assembly of Embryonic and Extraembryonic Stem Cells to Mimic Embryogenesis in Vitro. *Science 356*, eaal1810.
(12) Rivron, N. C., Frias-Aldeguer, J., Vrij, E. J., Boisset, J.-C., Korving, J., Vivié, J., Truckenmüller, R. K., van Oudenaarden, A., van Blitterswijk, C. A., and Geijsen, N. (2018) Blastocyst-like Structures Generated Solely from Stem Cells. *Nature 557*, 106−111.
(13) Elbert, D. L. (2011) Bottom-up Tissue Engineering. *Curr. Opin. Biotechnol. 22*, 674−680.
(14) Ovsianikov, A., Khademhosseini, A., and Mironov, V. (2018) The Synergy of Scaffold-Based and Scaffold-Free Tissue Engineering Strategies. *Trends Biotechnol. 36*, 348−357.
(15) Toda, S., Blauch, L. R., Tang, S. K. Y., Morsut, L., and Lim, W. A. (2018) Programming Self-Organizing Multicellular Structures with Synthetic Cell-Cell Signaling. *Science 361*, 156−162.
(16) Liu, J. S., and Gartner, Z. J. (2012) Directing the Assembly of Spatially Organized Multicomponent Tissues from the Bottom Up. *Trends Cell Biol. 22*, 683−691.
(17) Selden, N. S., Todhunter, M. E., Jee, N. Y., Liu, J. S., Broaders, K. E., and Gartner, Z. J. (2012) Chemically Programmed Cell Adhesion with Membrane-Anchored Oligonucleotides. *J. Am. Chem. Soc. 134*, 765−768.
(18) Dutta, D., Pulsipher, A., Luo, W., and Yousaf, M. N. (2011) Synthetic Chemoselective Rewiring of Cell Surfaces: Generation of Three-Dimensional Tissue Structures. *J. Am. Chem. Soc. 133*, 8704−8713.
(19) Luo, W., Pulsipher, A., Dutta, D., Lamb, B. M., and Yousaf, M. N. (2015) Remote Control of Tissue Interactions via Engineered Photo-Switchable Cell Surfaces. *Sci. Rep. 4*, 6313.
(20) Nose, A., Nagafuchi, A., and Takeichi, M. (1988) Expressed Recombinant Cadherins Mediate Cell Sorting in Model Systems. *Cell 54*, 993−1001.
(21) Friedlander, D. R., Mège, R. M., Cunningham, B. A., and Edelman, G. M. (1989) Cell Sorting-out Is Modulated by Both the Specificity and Amount of Different Cell Adhesion Molecules (CAMs) Expressed on Cell Surfaces. *Proc. Natl. Acad. Sci. U. S. A. 86*, 7043−7047.
(22) Katsamba, P., Carroll, K., Ahlsen, G., Bahna, F., Vendome, J., Posy, S., Rajebhosale, M., Price, S., Jessell, T. M., Ben-Shaul, A., et al. (2009) Linking Molecular Affinity and Cellular Specificity in Cadherin-Mediated Adhesion. *Proc. Natl. Acad. Sci. U. S. A. 106*, 11594−11599.
(23) Essen, L.-O., Mailliet, J., and Hughes, J. (2008) The Structure of a Complete Phytochrome Sensory Module in the Pr Ground State. *Proc. Natl. Acad. Sci. U. S. A. 105*, 14709−14714.
(24) Koo, H., Choi, M., Kim, E., Hahn, S. K., Weissleder, R., and Yun, S. H. (2015) Bioorthogonal Click Chemistry-Based Synthetic Cell Glue. *Small 11*, 6458−6466.
(25) Han, K., Go, D., Tigges, T., Rahimi, K., Kuehne, A. J. C., and Walther, A. (2017) Social Self-Sorting of Colloidal Families in Co-Assembling Microgel Systems. *Angew. Chem., Int. Ed. 56*, 2176−2182.
(26) Shi, P., Zhao, N., Lai, J., Coyne, J., Gaddes, E. R., and Wang, Y. (2018) Polyvalent Display of Biomolecules on Live Cells. *Angew. Chem., Int. Ed. 57*, 6800−6804.
(27) Todhunter, M. E., Jee, N. Y., Hughes, A. J., Coyle, M. C., Cerchiari, A., Farlow, J., Garbe, J. C., LaBarge, M. A., Desai, T. A., and Gartner, Z. J. (2015) Programmed Synthesis of Three-Dimensional Tissues. *Nat. Methods 12*, 975−981.
(28) Sato, K., Hosokawa, K., and Maeda, M. (2003) Rapid Aggregation of Gold Nanoparticles Induced by Non-Cross-Linking DNA Hybridization. *J. Am. Chem. Soc. 125*, 8102−8103.
(29) Sentürk, O. I., Chervyachkova, E., Ji, Y., and Wegner, S. V. (2019) Independent Blue and Red Light Triggered Narcissistic Self-Sorting Self-Assembly of Colloidal Particles. *Small 15*, 1901801.
(30) Zoltowski, B. D., Vaccaro, B., and Crane, B. R. (2009) Mechanism-Based Tuning of a LOV Domain Photoreceptor. *Nat. Chem. Biol. 5*, 827−834.
(31) Reichhart, E., Ingles-Prieto, A., Tichy, A. M., McKenzie, C., and Janovjak, H. (2016) A Phytochrome Sensory Domain Permits Receptor Activation by Red Light. *Angew. Chem., Int. Ed. 55*, 6339−6342.
(32) Vaidya, A. T., Chen, C.-H., Dunlap, J. C., Loros, J. J., and Crane, B. R. (2011) Structure of a Light-Activated LOV Protein Dimer That Regulates Transcription. *Sci. Signaling 4*, ra50.
(33) Mueller, M., Rasoulinejad, S., Garg, S., and Wegner, S. V. (2020) The Importance of Cell−Cell Interaction Dynamics in Bottom-Up Tissue Engineering: Concepts of Colloidal Self-Assembly in the Fabrication of Multicellular Architectures. *Nano Lett. 4*, 2257−2263.
(34) Yüz, S. G., Rasoulinejad, S., Mueller, M., Wegner, A. E., and Wegner, S. V. (2019) Blue Light Switchable Cell−Cell Interactions Provide Reversible and Spatiotemporal Control Towards Bottom-Up Tissue Engineering. *Adv. Biosyst. 3*, 1800310.
(35) Bugaj, L. J., Choksi, A. T., Mesuda, C. K., Kane, R. S., and Schaffer, D. V. (2013) Optogenetic Protein Clustering and Signaling Activation in Mammalian Cells. *Nat. Methods 10*, 249.
(36) Hörner, M., Raute, K., Hummel, B., Madl, J., Creusen, G., Thomas, O. S., Christen, E. H., Hotz, N., Gübeli, R. J., Engesser, R., et al. (2019) Phytochrome-Based Extracellular Matrix with Reversibly Tunable Mechanical Properties. *Adv. Mater. 31*, 1806727.
(37) Taslimi, A., Zoltowski, B., Miranda, J. G., Pathak, G. P., Hughes, R. M., and Tucker, C. L. (2016) Optimized Second-Generation CRY2-CIB Dimerizers and Photoactivatable Cre Recombinase. *Nat. Chem. Biol. 12*, 425−430.
(38) Yüz, S. G., Ricken, J., and Wegner, S. V. (2018) Independent Control over Multiple Cell Types in Space and Time Using Orthogonal Blue and Red Light Switchable Cell Interactions. *Adv. Sci. 5*, 1800446.
(39) Zhou, X. X., Zou, X., Chung, H. K., Gao, Y., Liu, Y., Qi, L. S., and Lin, M. Z. (2018) A Single-Chain Photoswitchable CRISPR-Cas9 Architecture for Light-Inducible Gene Editing and Transcription. *ACS Chem. Biol. 13*, 443−448.
(40) Nieman, M. T., Prudoff, R. S., Johnson, K. R., and Wheelock, M. J. (1999) N-Cadherin Promotes Motility in Human Breast Cancer Cells Regardless of Their E-Cadherin Expression. *J. Cell Biol. 147*, 631−644.
(41) Friedl, P., and Zallen, J. A. (2010) Dynamics of Cell-Cell and Cell-Matrix Interactions in Morphogenesis, Regeneration and Cancer. *Curr. Opin. Cell Biol. 22*, 557−559.
(42) McMillen, P., and Holley, S. A. (2015) Integration of Cell-Cell and Cell-ECM Adhesion in Vertebrate Morphogenesis. *Curr. Opin. Cell Biol. 36*, 48−53.
(43) Obana, M., Silverman, B. R., and Tirrell, D. A. (2017) Protein-Mediated Colloidal Assembly. *J. Am. Chem. Soc. 139*, 14251−14256.
(44) Li, F., Josephson, D. P., and Stein, A. (2011) Colloidal Assembly: The Road from Particles to Colloidal Molecules and Crystals. *Angew. Chem., Int. Ed. 50*, 360−388.
(45) Emond, M. R., Biswas, S., Blevins, C. J., and Jontes, J. D. (2011) A Complex of Protocadherin-19 and N-Cadherin Mediates a Novel Mechanism of Cell Adhesion. *J. Cell Biol. 195*, 1115−1121.
(46) Carpenter, A. E., Jones, T. R., Lamprecht, M. R., Clarke, C., Kang, I. H., Friman, O., Guertin, D. A., Chang, J. H., Lindquist, R. A., Moffat, J., et al. (2006) CellProfiler: Image Analysis Software for Identifying and Quantifying Cell Phenotypes. *Genome Biol. 7*, R100.
(47) Stauffer, W., Sheng, H., and Lim, H. N. (2018) EzColocalization: An ImageJ Plugin for Visualizing and Measuring Colocalization in Cells and Organisms. *Sci. Rep. 8*, 15764.
(48) Sheng, H., Stauffer, W., and Lim, H. N. (2016) Systematic and General Method for Quantifying Localization in Microscopy Images. *Biol. Open 5*, 1882−1893.

https://dx.doi.org/10.1021/acssynbio.0c00150
ACS Synth. Biol. 2020, 9, 2076−2086